
Two-Step Disentanglement for Financial Data

Naama Hadad¹, Lior Wolf^{1,2}, and Moni Shaha¹

¹Tel Aviv University, Israel

²Facebook AI Research

Abstract

In this work, we address the problem of disentanglement of factors that generate a given data into those that are correlated with the labeling and those that are not. Our solution is simpler than previous solutions and employs adversarial training in a straightforward manner. We demonstrate the new method on visual datasets as well as on financial data. In order to evaluate the latter, we developed a hypothetical trading strategy whose performance is affected by the performance of the disentanglement, namely, it trades better when the factors are better separated.

1 Introduction

Financial data analysis has attracted considerable attention in recent years, although the first quantitative models were presented almost fifty years ago. In the early 1970s Black and Scholes [3] gave the first formula for options pricing, where their theory was later extended by Merton [20]. For the microstructure of stock pricing, many models from economics [23], time series analysis [28] and random matrix theory [13] were applied. For an interesting survey on market microstructure and the statistical methods used to analyze it see [18].

A simplified model for stock price changes is that the price change can be decomposed into two factors, market movement and idiosyncratic movement. A common assumption is that the market return is Geometric Brownian motion, and cannot be predicted. However, since different stocks have different correlations with the market, one can neutralize the market factor from his portfolio. Since the correlations are non-stationary this market neutralizing needs to be done continuously, and the trading cost would make it too expansive.

It may be very interesting for prediction purposes and for data generation to be able to identify and separate factors that are relevant for our task from those which are not. One must bear in mind that, for financial data, simple economic factors, such as market correlation, sector correlation etc. explains only a small part of the variance, and more advanced statistical tools are needed. For a non-representing sample of economical and statistical methods applied to extract factors see: [2],[17],[26],[1] and others.

The problem of identifying factors and separating them from each other is not unique to economics. For example, in handwriting recognition, we would like to separate the factors that define the content of the text written from the factors that define its style. Having such separation can be used for improving identification models and for generation of written text. Other applications are speech recognition, creating realistic scenarios in computer graphics and others. The task of separating the factors that generated the observations is called *disentanglement*.

In this work, we present a new algorithm for disentanglement of factors, where the separation is based on whether the factors are relevant to a given classification problem. Following the terminology used in [19], we call the factors that are relevant for the classification task *specified factors*, and those which are not *unspecified factors*.

In order to perform disentanglement, we present a new adversarial technique. First, a classifier S is trained to predict the specified factors. The activations of S are then used to capture the specified component of each sample. A second network Z is then trained to recover the complimentary component. A first loss on Z ensures that the output of both networks together (S and Z) is able to reconstruct the original sample. A second loss, which is based on a third, adversarial, network, ensures that Z does not encode the specified factors. The algorithm makes very weak assumptions about the distribution of the specified and unspecified factors.

1.1 Related work

For the financial dataset, we briefly review two important models that we use.

CAPM model The capital asset pricing model (CAPM) [25] is one of the first quantitative models in finance theory. The model makes two assumptions: (i) one can invest in a risk-free asset of gain R_f (the risk free rate) and (ii) riskier assets have better expected compensation. We denote the average return of the market by R_m , and denote by R the return of the risky asset. Then, according to the model, the following linear relation holds:

$$\mathbb{E}[R] = R_f + \beta * (E[R_m] - R_f) \quad (1)$$

where $\beta = Cov(R, R_m)/Var(R_m)$, is the systematic risk of the asset compared to the market. Since this model was published there have been many works on fitting the parameters of this model on real data. For a discussion on the statistical aspects of the subject see [24].

Black-Scholes model The Black-Scholes model ([3], [20]) is a theoretical model for options pricing. It makes the following assumptions: (i) the market is continuous, free of commissions and permits short sell, (ii) you can borrow and lend money at the risk free rate and (iii) the market movements follow a Geometric Brownian motion.

Based on these assumptions, one can prove that if there are no arbitrage opportunities, then the price of an option with strike price S and time to expiration T is given by some formula that depends on the volatility. Intuitively, for a call option whose strike price is far above the current price, the probability that it would be exercised increases with the volatility. Hence, its price should be higher.

Disentanglement was studied in many contexts and has a vast literature. Early attempts to separate text from style using basic computer vision tools were made in [7]. In [27] voice data was analyzed. It was assumed that the data was generated by two sources and separated them using a bilinear model. In [6] manifold learning methods was used by ElGammal and Lee in order to separate the body configuration from the appearance. In recent years, few papers tackled this problem using neural networks. What-where encoders [10] combine the reconstruction criteria with the discrimination in order to separate the factors that are relevant for the labels. In [11] variational auto encoders were used to separate the digit from the style. However their approach can not generalized to unseen identities. This restriction was relaxed in [19], where they trained a conditional generative model by using an adversarial network to remove label information from the unspecified part of the encoding.

Concurrently with our work, the Fader Networks [14] employ an architecture that is closely related to the second step of our two-step architecture. While in our model a classifier is trained to capture the specified factors, in the architecture of [14], the labels are used directly. The main advantage of our architecture in comparison to the one step alternative, is the support of novel labels at test time, i.e., it is not limited to the set of labels seen during training. This is crucial in our modeling for financial data, where the specified factors (the labels) denote the market behavior during train years, and the test years differ from the train ones.

Generative Adversarial Networks GAN [9] is a method to train a generator network G that synthesizes samples from a target distribution given noisy inputs. In this approach, a second network called the discriminator D in jointly trained to distinguish between generated samples and data samples. This ‘‘competition’’ between the generator and the discriminator, induces a zero-sum game whose equilibrium is reached when the discriminator can no longer distinguish between the generated samples and the empirical ones. Since this approach was published, many variations on the basic idea appeared, see for example [21], [5], [4].

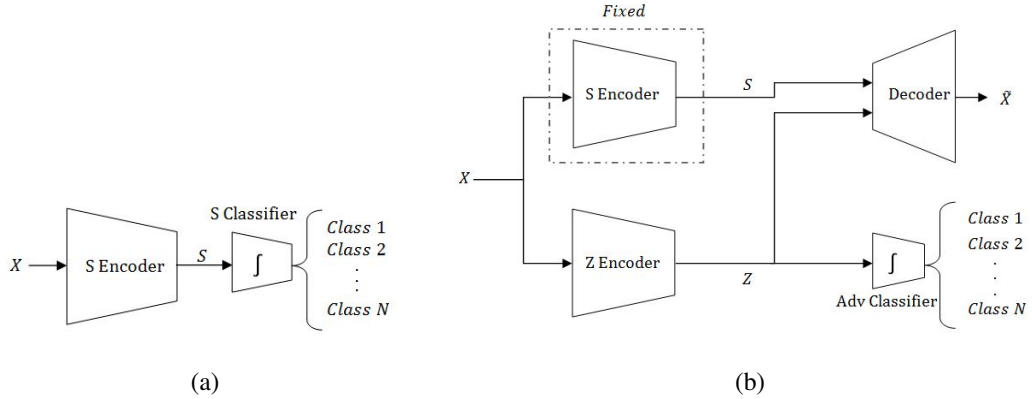


Figure 1: Network architecture: (a) We train the S encoder and its classification network on a pure classification task (b) Once S is given, we freeze S weights and train the Enc-Dec network and the adversarial classifier alternatively

2 Method

The Problem of Disentanglement We are given a set of labeled inputs X with the matching labels Y . Our goal is to represent the data using two disjoint parts of a code, S , and Z . We require S to contain all the information relevant for the class ids Y , and Z to contain only the unspecified factors of the data. For the example of handwriting recognition, if Y is the text written in the image samples X , then S will contain the information about the textual content Y , whereas Z will only contain information about the style of writing.

The Model For the encoding, we chose S and Z to be vectors of real numbers rather than a one-hot vector. This idea, presented in [19], enables the network to generalize to identities that were not represented in the training set.

We define a new network architecture for the disentanglement of the factors. Our architecture is simpler and more straightforward than the one presented in [19]. The network contains two deterministic encoders to map X to its specified and unspecified components $S = Enc_S(X)$ and $Z = Enc_Z(X)$ accordingly. To train the S encoder Enc_S , we first use a sub-network for the classification task and train the S classifier concurrently with Enc_S . This sub-network accepts X as its input, encodes it to a vector S , and then runs the S classifier on S to obtain the labels Y , see Fig. 1(a). The result of this network is an encoding of the data that contains the information needed in order to predict the class identity.

In a second step, Enc_S is kept fixed. To train the Z -encoder to ignore the specified factors and contain data only on the unspecified factors, we use a new variation of adversarial networks. The configuration of the network is given in Fig 1(b), and it is composed out of two network branches. The adversarial classifier (see the bottom part of the figure) is being trained to minimize the classification loss given Z, Y as input, namely, it is trained to classify Z to Y . The Enc-Dec network (the rest of the network) is trained to minimize the sum of two terms: (i) the reconstruction error (given S and Z), and (ii) minus the adversarial network loss.

More formally, let θ_Z be the parameters of $Enc_Z(X)$ and let θ_X be the parameters of the reconstruction network with output $\tilde{X} = Dec(S, Z)$. Let θ_A be the parameters of the adversarial network. We define $L_{adv}(\{(Z, Y)\}, \theta_A)$ to be the classification loss of the adversarial network and $L_{rec}(\{S, Z, X\}, \theta_X)$ to be the reconstruction loss of \tilde{X} . When optimizing θ_A , L_{adv} is minimized. When optimizing the two other networks, θ_Z and θ_X , the objective is to simultaneously minimize L_{rec} and maximize L_{adv} . Hence, our objective is:

$$\min_{\theta_Z, \theta_X} \{L_{rec} - \lambda * L_{adv}\}, \lambda > 0 \quad (2)$$

Note that while GANs are typically used in order to improve the quality of generated output such as images, here we use an adversarial configuration to encourage the encoding to "forget" information about the labels, which, in turn, leads to the disentanglement.

Training the S encoder together with the Z encoder and the subsequent decoder, could lead the network to converge to a degenerated solution, where all information is encoded in S , whereas Z holds no information on any factor. By training the S network in the first stage, and then fixing the values of its parameters, this scenario is avoided. Since S has a limited capacity it ignores most of the information on the unspecified factors, that is irrelevant for its goal.

Training details We employ MSE for the L_{rec} loss, and use categorical cross-entropy loss for both the S classifier's loss and L_{adv} . The λ for each dataset was chosen independently using few iterations on validation data.

For the training of the S -network and the Enc-Dec network, we apply the Adam optimization method [12] with a learning rate of 0.001 and beta of 0.9. For the adversarial classifier, we used SGD with a learning rate of 0.001.

While training the Z -network, we have noticed that the adversarial part requires more steps to stabilize, since it should solve a complicated classification task on a changing input. Therefore, we run, at each iteration, one mini-batch to train the Enc-Dec network, followed by three mini-batches to train the adversarial network.

2.1 Comparison to [19] on Synthetic data

To illustrate the advantages of our approach in comparison to the more involved method of [19], we generated images of a gray rectangle on a white or black background. We refer to the background color as the unspecified factor Z , whereas the location of the rectangle is the specified factor S . We denote the ten possible values of S by $\{s_0, \dots, s_9\}$. All possible twenty images were drawn with equal probability.

We also generated similar images, where the unspecified factor consists of two binary variables - the first controls the upper half background color and the second controls the lower half background color. All forty images were drawn with equal probability.

We refer to the sets as *Synth1* and *Synth2*. For the encoding, we chose both S and Z to be vectors of size 4. We run our network and the network in [19] to obtain S, Z for *Synth1* and *Synth2*. We then used a neural network classifier with three dense layers of size 8 on S to find the label. The obtained accuracy was 100% for both networks.

We then examined the Z vectors that were obtained from both methods of disentanglement on *Synth1* and *Synth2*. First we verified using a classifier that the background color can be inferred from Z perfectly, whereas inferring the location of the rectangle from Z leads to accuracy that is close to random. Next we turned to examining the distribution of Z for *Synth1* and *Synth2*, these distributions are presented in Fig. 2,3 respectively. The figures show the values of the components Z_0, \dots, Z_3 for all of the data points. Each color represents a different value of the latent variable Z . Note that since the method in [19] defines Z to be a random vector drawn from a normal distribution specified by μ, σ , we show a sample of the drawn Z vectors.

For the binary case (*Synth1*, Fig. 2) our encoding shows two narrow peaks well separated in Z_3 , whereas all other components have one peak (the coordinate that contains the information is completely arbitrary since all coordinates are treated the same way). In the VAE encoder, the information was separated only for Z_0 , but even the best classifier (which is LDA in this case) will have some error, since the peaks were not disjoint. This simple experiment also demonstrates that our results are simpler to understand.

The gap in the explicitness of the results, as encoded in Z is more apparent on *Synth2*. In Fig. 3, we see that our encoding of Z is well separated on Z_0, Z_1 while in the other method, one cannot tell the number of values without further analysis or prior knowledge about Z . Moreover, applying standard PCA on the sampled Z vector of the auto encoder, gave four components with similar variance, as shown in Tab. 1.

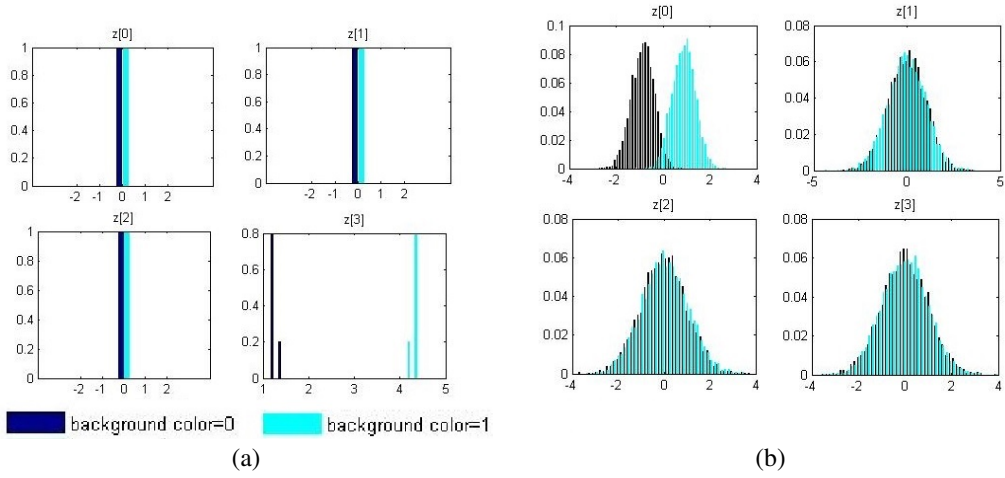


Figure 2: Synthetic data: Unspecified factor of dimension 1 (a) Z different components histogram for the encoding from our model (b) Z different components histogram for the encoding from [19] model.

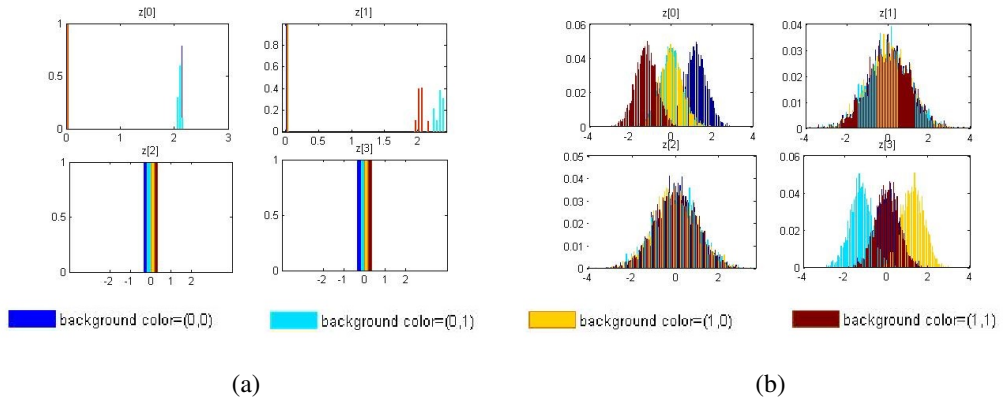


Figure 3: Unspecified factor of dimension 2 (a) The different components of Z for the encoding from our model. (b) An histogram of the different components of Z for the encoding from the model of [19].

3 Experiments

We evaluate our method on a few visual disentanglement benchmarks from the literature, as well as on simulated and real financial data.

The detailed network architecture used for each of the experiments is described in Tab. 2

Table 1: Z PCA components explained variance for unspecified factor of dimension 1 and 2

PCA component:	<i>Synth1</i>				<i>Synth2</i>			
	1	2	3	4	1	2	3	4
Our model	1.000				0.610	0.390		
[19]	0.252	0.251	0.25	0.247	0.263	0.249	0.248	0.240

Table 2: Network architecture

	MNIST,Sprites	NORB,Extended YaleB	Stocks return
Encoders S,Z	Three 5x5 convolutional layers with stride 2 and a dense S/Z dimension layer. all with ReLU non-linearities	Three 3x3 convolutional layers with stride 2 and a dense S/Z dimension layer. all with ReLU non-linearities.	4 dense layers of sizes 100,66,66,50 with ReLU non-linearities
S classifier	3 dense layers x 256 hidden units, Batch Normalization, ReLU and a softmax for the output	2 dense layers x 16 hidden units, Batch Normalization, ReLU and a softmax for the output	2 dense layers x 50 hidden units, Batch Normalization, ReLU and a softmax for the output
Decoder	Mirroring network to the encoders: dense layer and three convolutional network with upsampling	Mirroring network to the encoders: dense layer and three convolutional network with upsampling	4 dense layers of sizes 70,66,66,100 with ReLU non-linearities
Adversarial Classifier	3 dense layers x 256 hidden units, Batch Normalization,ReLU and a softmax for the output	3 dense layers x 256 hidden units, Batch Normalization, ReLU and a softmax for the output	3 dense layers x 50 hidden units, Batch Normalization, ReLU and a softmax for the output
S, Z #dims	Mnist: 16,16 Sprites: 32,128	32,256	20,50

3.1 Literature benchmarks

We followed a previous work [19] and tested our model on four visual datasets - MNIST [15], NORB [16], Sprites dataset [22] and the Extended-YaleB dataset [8].

For measures of performance on the visual datasets, we also followed the ones suggested in [19]. Note that all these measures are subjective.

- *Swapping* - In swapping, we generate an image using S from one image, I_1 , and Z from a different image, I_2 . In a good entanglement, the resultant image preserves the S -qualities of I_1 and the Z -qualities of I_2 .
- *Interpolation* - Interpolation of two source images is a sequence of images generated by linearly interpolating the S and Z components of the two different sources. The measure is again done by visual judgment of the resultant images. i.e., we expect to see "more" of the look of the second image, the bigger its weight gets. Interpolation is done in both the S space and the Z space.
- *Retrieval* - In order to assess the lack of correlation between the S and Z components, we perform a query based on either the S part or the Z part, in each case retrieving its nearest neighbors in its corresponding space.
- *Classification Score* - In addition to the qualitative measures above, in this measure we try to quantify the amount of information on the class that each part of the data (S and Z) contains. Since measuring this directly is a difficult task, we approximate it by running a classification algorithm. A good disentanglement is such that when running the classifier on the S part gives high accuracy, whereas when running it on the Z part gives nearly random results.

MNIST - For the MNIST data, the S part is the digit and the Z part is the style. In Fig. 4, we present the results for swapping and interpolation. The rows of the table in the left hand side of the figure shows the style (Z) and the columns the digit. To the best of our judgment, the style looks well separated from the content.

Sprites dataset - This dataset contains color images of sprites [22]. Each sprite character is defined by body type, gender, hair type, armor type, arm type and greaves type. Overall there are 672 different characters, from which we use 572 characters for the training set and 100 characters for the test set. For each character, there are five animations each from four viewpoints, each animation has between 6 and 13 frames. We use character's identity as the specified component. The results from swapping and interpolation are shown in Figure 5. Our model learned to separate the character from its position and weapon and generalizes the separation to unseen characters.

Examining the retrieval results in Fig. 6, it is possible to see that for the Z part (sub-figure (b)), the characters in any row is random but its pose is kept. In the S part (sub-figure (a)), the character is perfectly kept, whereas the pose is not. In [19], it seems that Z holds some information on S because the hair style and color rarely changes between characters.

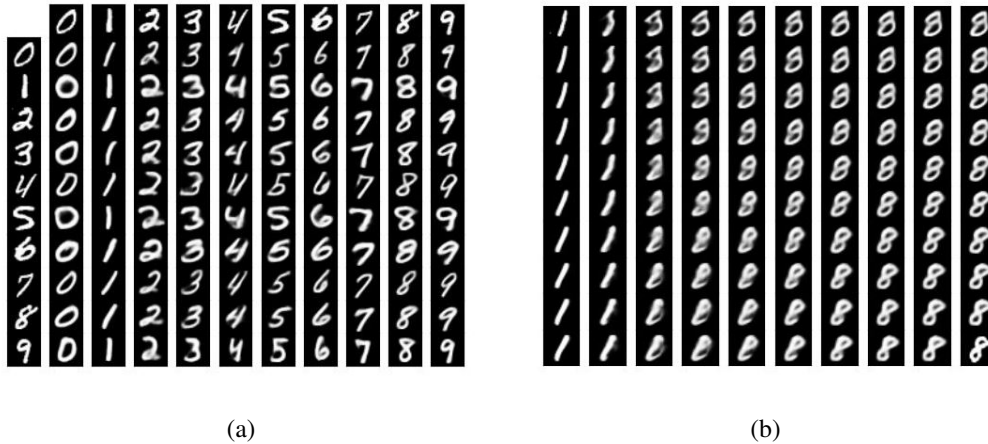


Figure 4: (a) swapping the specified and unspecified components of MNIST images. The images are generated using Z from the left column and S from the top row in the decoder. The diagonal digits show reconstructions. (b) Interpolation results. the images in the top-left and bottom-right corners are from the test set. The other digits are generated by interpolation of S and Z gradually. Z interpolate along the rows and S through the columns.

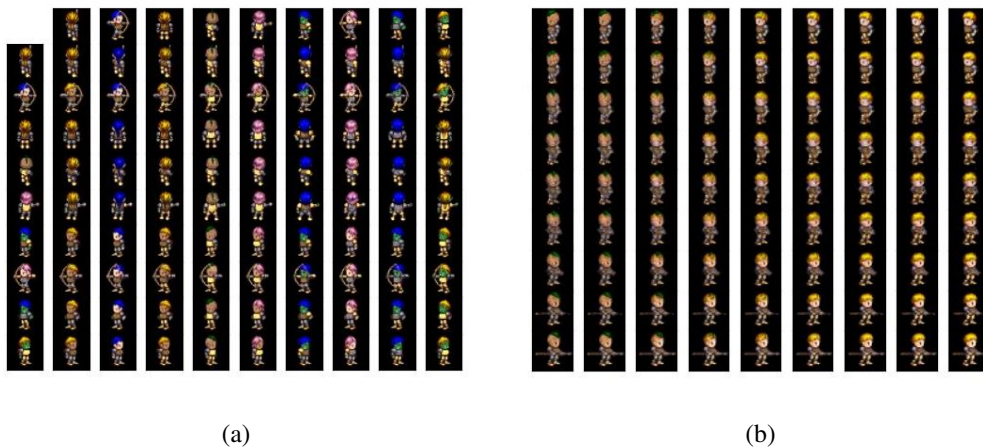


Figure 5: (a) Swapping the specified and unspecified components of Sprites images. The images are generated using Z from the left column and S from the top row in the decoder. (b) Interpolation results. the images in the top-left and bottom-right corners are from the test set. The other digits are generated by gradual interpolation of S and Z . Z interpolates along the rows and S through the columns.

Small NORB dataset [16] - The NORB dataset contains images of 50 toys belonging to five generic categories: four-legged animals, human figures, airplanes, trucks, and cars. The objects were imaged by two cameras under six different illumination conditions, nine elevations and 18 azimuths. The training set is composed of five instances of each category and the test set of the remaining five instances. We use the instance identity as the specified component and have 25 different labels for the training set.

The swapping results were not perfect. We succeeded in separating different azimuths and background from the instance. However, for some of the categories, the reconstruction contained mistakes. This is probably due to the high variability between the instances in the train and the test. The numerical results give some hint that this is the case, because our train and test errors were very different.



Figure 6: Sprites dataset retrieval results (a) Querying on the specified component S . (b) Querying on the unspecified component Z . The components of the sprites on the left column are used as the query.

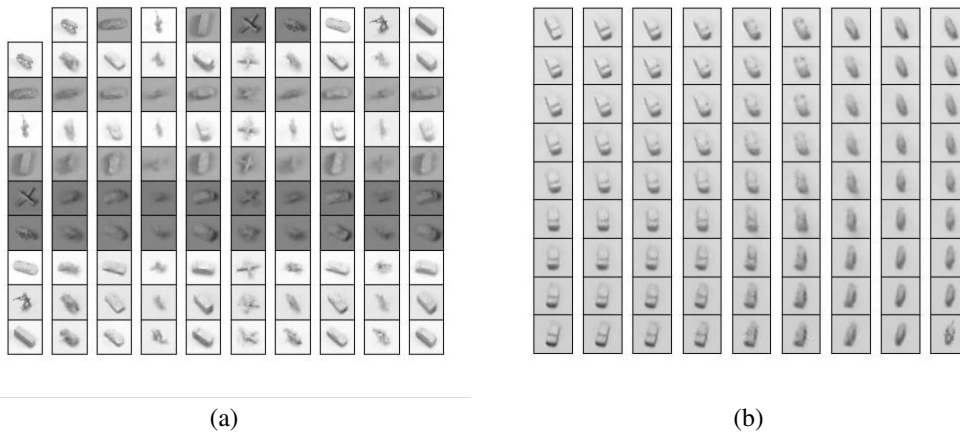


Figure 7: (a) Swapping the specified and unspecified components of the NORB test set images. (b) Interpolation results. These are the same arrangements as in Figure 5.

The results look good for the interpolation, see Figure 7. A similar degradation of results was also observed in [19]

Extended-YaleB [8] - The extended-YaleB Face dataset contains 16095 images of 28 human subjects under nine poses and 64 illumination conditions. The training set contains 500 images per subject, while the test contains roughly 75 images per subject. We use subject identity as the specified component.

Results for swapping and interpolation for images from the test set shown in Figure 8. For swapping, one can see that illumination conditions are transferred almost perfectly, whereas the position is not perfectly transferred (see for example line 6, column 5). We again suspect that this is mainly because some of the positions were missing in the training set, and with more data we expect the results to improve. For the interpolation, some of the mixed identities do not resemble each of the sources.

Quantitative results The numerical results for all datasets are shown in Table 3. One can see that the unspecified component is almost agnostic to the identity, while the classifier on the specified component achieves high accuracy. For comparison with [19], we added to the table the results that were reported in that paper. For most of the cases, our model achieves higher accuracy for S . This is



Figure 8: (a) Swapping the specified and unspecified components of Yale test set images. (b) Interpolation results. These are the same arrangements as in Figure 4. In this case, the results are visibly inferior to the examples presented in [19].

Table 3: Classification error rate based on S or Z for our model and as reported in [19]. *While [19] reports 60.7% chance, we observe 56% in the test set, and 67% in the train set.

	Mnist		Sprites		NORB		Extended-YaleB	
	Z	S	Z	S	Z	S	Z	S
Our (train)	87.0%	0.1%	66.0%	0.0%	78.9%	1.1%	95.7%	0.00%
Our (test)	87.0%	0.8%	58.0%	0.0%	79.2%	15.2%	96.3%	0.00%
[19] (train)	-	-	58.6	5.5%	79.8%	2.6%	96.4%	0.05%
[19] (test)	-	-	59.8	5.2%	79.9%	13.5%	96.4%	0.08%
Random-chance	- 90.0% -		- * -		- 80.0% -		- 96.4% -	

expected, since we train the S -encoder for classification. As for the unspecified component Z , our performance on the train and the test set are similar, except for the NORB dataset where our error rate is slightly worst. For this dataset, the error rate of S in the test set is much larger than that of the train set, and in [19] they explain this result by overfitting. Note that for this dataset, there are only five training instances per category, which makes generalization difficult.

3.2 Results on Simulated CAPM Data

In order to verify our evaluation measures we generated a synthetic data-set that followed the CAPM assumptions and checked how well can we learn the stock specific information and the market return from S, Z . The results, shown below, show that Z holds the information about the β -groups and almost no information about the $E[R_m]$, whereas S holds the complementary information.

The Simulation - We synthesize data as offered based on the CAPM model as follows. We define 150 periods of 50 days for training. For each period, we draw the following:

- R_f - period risk free rate, distributed $U[0.0025, 0.03]$.
- $E[R_m]$ - daily market return for this quarter, $R_f/50 + 0.04/50 * N(0, 1)$.
- R_m - market return vector, the day return that is drawn from $E[R_m] + 0.0005 * N(0, 1)$.
- β - betas for 1500 assets in this period, distributed $U[-1, 3]$.

For each stock, X is calculated as $R_f/50 + \beta(R_m - R_f/50) + \epsilon$, where ϵ is distributed $0.0005 * N(0, 1)$, concatenated to the R_m vector, plus added noise in order to encourage generalization.

Evaluation - Using a PCA decomposition of size two for Z , X and S and running logistic regression to classify the results to four beta groups, we get accuracy of 64%, 40% and 33% respectively. We can see that, as expected, Z holds the information about the beta, which is stock specific. S accuracy is also much lower than Z accuracy.

On the other hand, using the same PCA components to deduce $E[R_m]$ we get accuracy of 33%, 96% and 95% for Z , X and S . As expected, since $E[R_m]$ is drawn per period, it belongs to the specified factors and is mostly included in S .

Optimizing [18] on the same data we obtain accuracy of 54% and 37%, trying to classify beta (unspecified) based on Z and S respectively and 75%, 95% accuracy for R_m (unspecified) based on Z , S . This is additional evidence that our method outperforms [18]. As desired, our Z is better at classifying beta and worse at classifying the specified factor and our S is also worse at classifying beta.

3.3 Results on Financial Data

We applied our model on the daily returns of stocks listed in NASDAQ, NYSE and AMEX, from the Center for Research in Security Prices (CRSP) database. For all datasets, the results were measured on the test set.

The Data - We used daily returns of stocks from the Nasdaq, NYSE and AMEX exchanges. The training set consists of the years 1976-2009 and the test set 2010-2016. Each year is divided into four quarters of approximately 63 trading days. As an input to the network, we used for each stock the returns of the first 50 days of each quarter, as well as the market returns for the same 50 days. In order to improve generalization, we added ϵ_i a random noise $N(0, 0.0016)$.

The goal of the disentanglement is to separate market behavior from specific stock's movements. In order to do so, we labeled each quarter in the training set differently, in order to have 136 such labels. Next, we let S encode the label information and Z encode all the rest of the information. To give further motivation for this decomposition, we assume a hypothetical world where the CAPM model is exact. An optimal representation would be that Z encodes β and S encodes the risk-free interest rate R_f , as well as the market movements. Note that the adversarial part cannot reconstruct the market returns from β , but the decoder can perfectly reconstruct the stock and market returns based on the CAPM model.

We chose the encoding, so that the S -part is a vector of length 20, and the Z -part is a vector of length 50. The other parameters of the network are outlined in the appendix.

Evaluation - The assessment of the results in this dataset is not straightforward, since the CAPM model is far from being exact. Furthermore, stocks returns are known to be highly non-stationary and their market correlation is not deterministic. Therefore, we adopt two indirect metrics, (i) checking the stock specific information from Z and (ii) evaluating a trading strategy based on the predictions that came from Z .

For a sanity check, we start by showing that S contains market information. We did a PCA on the S -part of the encoding and examined the first component. This component was correlated with the average return of the market during the tested period. Checking the correlation coefficient between the market return on the test period and the first component of the PCA is 0.55.

We then defined a few stock specific measures. For each of them, we built three classification models, the first gets as input X , the second gets Z and the third gets S . Note that although X contains all the information in Z and maybe more, if we train a classification model with low complexity, then using Z which encodes relevant information from X would give better results.

For each stock, we calculated β and the correlation coefficient ρ with the market during the last year. We constructed a discrete version of these measures with four classes each. The classifier we used is logistic regression, since it is often used in the econometrics literature, and it also gave good results on the synthetic CAPM-generated data. The predictive accuracy on the test set for each of the six models (2 measures times 3 inputs) is given in Table 4. From this table, we clearly see that we failed to reveal stock properties from X and S , but managed to do it from Z .

A very important measure that can be used in options trading is the volatility. Using a model on Z , we predicted the next day and next 5-days volatility. The results are given in Table 6. The accuracy

Table 4: Logistic regression accuracy for β, ρ

	beta	rho	beta [19]	rho [19]
Z	35%	31%	31%	30%
S	26%	26%	28%	28%
Raw	26%	26%		
Rand	25%	25%	25%	25%

Table 5: Options portfolio return. The mean, Std and percent of trading days with positive return

	Mean	SD	Traded days %
Z (Ours)	3.1%	0.026	89.3%
Z [19]	2.9%	0.039	78.6%
X	2.6%	0.030	78.6%

Table 6: Logistic regression accuracy for next day/week volatility. The rightmost column is the results of the model presented in [19]. Other columns are the results of our model.

	NY	AM	NQ	All	[19]
Z-1	31%	37%	30%	31%	30%
S-1	26%	24%	24%	25%	27%
X-1	28%	24%	24%	—	25% —
Rnd-1	—	—	25%	—	—
Z-5	40%	49%	36%	39%	34%
S-5	26%	27%	25%	26%	30%
X-5	25%	29%	25%	—	26% —
Rnd-5	—	—	25%	—	—

of the different models changes between the stock groups, but the performance is significantly better for the model based on Z .

The volatility is an important component in options pricing models, such as Black-Scholes model [3]. We developed the following theoretical options trading strategy:

- We estimated the volatility of a stock, based on its volatility in the last fifty trading days.
- We run a classification model for the stock, based on either X or Z
- For the ten stocks whose predicted volatility minus measured volatility is the highest, we bought a put and a call option. Similarly for the ten stocks whose predicted volatility minus measured volatility is the lowest, we sold one put option and one call option. The strike price of the options is 5% higher than the current price. The time to expire is 60 days for the high predicted volatility options and 5 days for the low volatility ones.
- We cleared our position on the next day, i.e., sold, if we bought options yesterday and vice-versa.

Note that this strategy is market neutral and relies only on volatility. We are aware of the fact that we ignored trading cost, liquidity and other technicalities that make this strategy unrealistic. However, we used it as a way to compare the classifier that used X to the one that used Z as input. The results are summarized in Table 5. As one can see, using Z is better.

As a concluding remark for this section, we tried using the algorithm in [19] on this data and repeated our measures. We made a best effort to optimize the parameters, and still obtained inferior results in terms of our measures. However, we cannot overrule the possibility that with more calibrations we would get better results. The results from [19] for financial data are presented next to ours in tables 4, 6 and 5. It can be seen that our accuracy and portfolio performance based on Z are better and we also achieved better separation from S , since it is almost agnostic to specific stock properties.

4 Conclusions

This paper presents a simple architecture for solving the problem of disentanglement. Given labeled data, our algorithm encodes it as two separate parts, one that keeps the information regarding the labels and the other that is agnostic to the labels. We tested the network on visual and financial data, and found that it performed well, compared to a leading literature method. Our architecture does not assume a distribution on the unspecified factors and the resultant encoding seemed both more interpretable as well as more suitable as a representation for learning various unspecified qualities.

References

- [1] Andrew D Back and Andreas S Weigend. A first application of independent component analysis to extracting structure from stock returns. *International journal of neural systems*, 8(04):473–484, 1997.

- [2] Christopher M Bilson, Timothy J Brailsford, and Vincent J Hooper. Selecting macroeconomic variables as explanatory factors of emerging stock market returns. *Pacific-Basin Finance Journal*, 9(4):401–426, 2001.
- [3] Fischer Black and Myron Scholes. The pricing of options and corporate liabilities. *Journal of Political Economy*, 81(3):637–54, 1973.
- [4] Duan Yan Houthoof Rein Schulman John Sutskever Ilya Chen, Xi and Pieter. Abbeel. Infogan: Interpretable representation learning by information maximizing generative adversarial nets. In *Advances in neural information processing systems*, pages 2172–2180, 2016.
- [5] Emily L Denton, Soumith Chintala, Rob Fergus, et al. Deep generative image models using a laplacian pyramid of adversarial networks. In *Advances in neural information processing systems*, pages 1486–1494, 2015.
- [6] Ahmed Elgammal and Chan-Su Lee. Separating style and content on a nonlinear manifold. In *Computer Vision and Pattern Recognition, 2004. CVPR 2004. Proceedings of the 2004 IEEE Computer Society Conference on*, volume 1, pages I–I. IEEE, 2004.
- [7] Lloyd A. Fletcher and Rangachar Kasturi. A robust algorithm for text string separation from mixed text/graphics images. *IEEE transactions on pattern analysis and machine intelligence*, 10(6):910–918, 1988.
- [8] Athinodoros S. Georghiades, Peter N. Belhumeur, and David J. Kriegman. From few to many: Illumination cone models for face recognition under variable lighting and pose. *IEEE transactions on pattern analysis and machine intelligence*, 23(6):643–660, 2001.
- [9] Ian Goodfellow, Jean Pouget-Abadie, Mehdi Mirza, Bing Xu, David Warde-Farley, Sherjil Ozair, Aaron Courville, and Yoshua Bengio. Generative adversarial nets. In *NIPS*, pages 2672–2680. 2014.
- [10] Fu Jie Huang, Y-Lan Boureau, Yann LeCun, et al. Unsupervised learning of invariant feature hierarchies with applications to object recognition. In *Computer Vision and Pattern Recognition, 2007. CVPR'07. IEEE Conference on*, pages 1–8. IEEE, 2007.
- [11] Diederik P Kingma, Shakir Mohamed, Danilo Jimenez Rezende, and Max Welling. Semi-supervised learning with deep generative models. In *Advances in Neural Information Processing Systems*, pages 3581–3589, 2014.
- [12] D.P. Kingma and J. Ba. Adam: A method for stochastic optimization. In *The International Conference on Learning Representations (ICLR)*, 2016.
- [13] Laurent Laloux, Pierre Cizeau, Jean-Philippe Bouchaud, and Marc Potters. Noise dressing of financial correlation matrices. *Physical review letters*, 83(7):1467, 1999.
- [14] Guillaume Lample, Neil Zeghidour, Nicolas Usunier, Antoine Bordes, Ludovic Denoyer, and Marc Aurelio Ranzato. Fader networks: Manipulating images by sliding attributes. *CoRR*, abs/1706.00409, 2017.
- [15] Yann LeCun and Corinna Cortes. MNIST handwritten digit database. 2010.
- [16] Yann LeCun, Fu Jie Huang, and Leon Bottou. Learning methods for generic object recognition with invariance to pose and lighting. In *Computer Vision and Pattern Recognition, 2004. CVPR 2004. Proceedings of the 2004 IEEE Computer Society Conference on*, volume 2, pages II–104. IEEE, 2004.
- [17] Sydney C Ludvigson and Serena Ng. Macro factors in bond risk premia. *Review of Financial Studies*, 22(12):5027–5067, 2009.
- [18] Ananth Madhavan. Market microstructure: A survey. *Journal of financial markets*, 3(3):205–258, 2000.

- [19] Michael F Mathieu, Junbo Jake Zhao, Junbo Zhao, Aditya Ramesh, Pablo Sprechmann, and Yann LeCun. Disentangling factors of variation in deep representation using adversarial training. In D. D. Lee, M. Sugiyama, U. V. Luxburg, I. Guyon, and R. Garnett, editors, *Advances in Neural Information Processing Systems 29*, pages 5040–5048. Curran Associates, Inc., 2016.
- [20] Robert C Merton. Theory of rational option pricing. *The Bell Journal of economics and management science*, pages 141–183, 1973.
- [21] Alec Radford, Luke Metz, and Soumith Chintala. Unsupervised representation learning with deep convolutional generative adversarial networks. *arXiv preprint arXiv:1511.06434*, 2015.
- [22] Scott E Reed, Yi Zhang, Yuting Zhang, and Honglak Lee. Deep visual analogy-making. In *Advances in Neural Information Processing Systems*, pages 1252–1260, 2015.
- [23] Richard Roll. A simple implicit measure of the effective bid-ask spread in an efficient market. *The Journal of Finance*, 39(4):1127–1139, 1984.
- [24] Jay Shanken. On the estimation of beta-pricing models. *The review of financial studies*, 5(1):1–33, 1992.
- [25] O. William Sharpe and Merton Miller. Capm. *Equilibrium*, 1964.
- [26] James H Stock and Mark W Watson. Implications of dynamic factor models for var analysis. Technical report, National Bureau of Economic Research, 2005.
- [27] Joshua B Tenenbaum and William T Freeman. Separating style and content. *Advances in neural information processing systems*, pages 662–668, 1997.
- [28] Ruey S Tsay. *Analysis of financial time series*, volume 543. John Wiley & Sons, 2005.